COMMUNICATIONS
FROM THE
KONKOLY OBSERVATORY
OF THE
HUNGARIAN ACADEMY OF SCIENCES

MITTEILUNGEN
DER
STERNWARTE
DER UNGARISCHEN AKADEMIE
DER WISSENSCHAFTEN

BUDAPEST — SZABADSÁGHEGY

No. 85.

L. G. BALÁZS, M. PAPARÓ, I. TÓTH

DISTRIBUTION OF STARS OF SPECTRAL TYPES OF F7 AND EARLIER IN A FIELD AROUND NGC 7686

BUDAPEST, 1985

ISBN 963 8361 21 2
HU ISSN 0324 — 2[illegible]4

Felelős kiadó: Szeidl Béla

Hozott anyagról sokszorosítva

8616202 MTA Sokszorosító, Budapest. F. v.: dr. Héczey Lászlóné

DISTRIBUTION OF STARS OF SPECTRAL TYPES OF F7 AND EARLIER IN A FIELD AROUND NGC 7686

ABSTRACT

A statistical study was performed on 993 stars of spectral type F7 and earlier in 19.5 sq. deg. field centred on NGC 7686 down to a limiting magnitude of 12.5. The observational material was obtained with Konkoly Observatory's 60/90/180 cm Schmidt telescope. The stars were classified utilizing small scale spectra (580 Å/mm at Hγ) and photographic UBV colours were measured. The interstellar absorption in this area was determined to be A_v = 1.2 mag. and the space densities in the spectral groups of B8-A1, A2-A3, A4-A7, A8-F2 and F3-F7 were obtained using the matrix method of Dolan. Our empirical space distributions were compared with an exponential model, with Camm's models, with Bahcall's model and with that of Woolley and Stewart. The best fit was obtained by an isothermal model and this fitting enabled us to estimate the total mass density near the Sun resulting 0.104 $M_\odot/pc^3$ using the B8-A1 group and 0.159 $M_\odot/pc^3$ using the A type stars. These figures do not differ from the observed total mass density on the one sigma significance level.

INTRODUCTION

The present work is a continuation of the combined spectral and multicolour investigation of stars of spectral types of F7 and earlier at intermediate galactic latitudes. In two previous papers (*Balazs 1975, Paparo and Balazs 1982*,hereafter referred to as Paper I and Paper II, respectively) we found further evidence to those reported in the literature (see references in Paper I), that the space distribution of A type stars is composed of two kinematically different subsystems resulting in an inflexion point on the log-density curve at about 200 pc above the galactic plane. On combining the results of other authors with our own measurements, we found (see Paper I) that the density ratio at z=0 of the two subsystems depends on spectral type and displays a jump at about AO. We interpreted this jump as a consequence of discontinuous star formation in the region surveyed (r<1000 pc from the Sun). It is thought that this jump might result from the passage of the density wave through the solar neighbourhood. The life times of these stars at which the jump appeared enabled us to estimate the period between two

consecutive increases of star formation activity. It turned out to be of 1×10^8 years $< \tau < 6 \times 10^8$ years.

Discontinuous star formation followed by dynamic evolution could account for the shape of the spatial distribution of the stars perpendicular to the galactic plane. Recent investigations (*Wielen 1977, Wielen and Fuchs 1983, Villumsen 1984, Lacey 1984, Palous and Piskunov 1985*) have confirmed the result of *Spitzer and Schwarzschild (1953)* that the dynamic evolution of stellar spatial and kinematic distributions could proceed fast enough to be significant during the period mentioned above. Thus, in addition to discontinuous star formation, this is an important phenomenon in interpreting the spatial distribution of stars having life times in the order of 10^8 years, i.e. of the A type stars. The significance of the spatial distribution of A type stars in studying star formation periods and dynamic evolution has been emphasized by *Balazs (1977,1984)*.

It is important to prove that the space distribution of A type stars observed is really due to the processes mentioned above. To exclude the possibility that the observed characteristics represent a local phenomenon only, one should extend the investigations as far from the Sun as possible. Since the inflexion point appears at about 200 pc above the galactic plane, one has to make observations at intermediate or low galactic latitudes in order to extend the domain of investigations. This was an important motivation for selecting the galactic latitudes of our investigations in Papers I and II. The area presently surveyed has a somewhat lower latitude, of 11.63 degrees.

OBSERVATIONAL MATERIAL

We have investigated an area of 19.5 sq.deg. centred on l=109.52 deg. , b=11.63 deg. (alpha=$23^h27.8^m$, delta=$48^o51'$). The observations were carried out with the 60/90/180 cm Schmidt telescope of the mountain station of Konkoly Observatory. We obtained spectral types and UBV colours for 993 stars down to 12.5 photographic magnitude. For spectral classification we used

three objective prism plates taken with a 5 deg. UBK7 (UV transmitting) prism that gives a dispersion of 580 Å/mm at $H\gamma$. The widening and the exposures were the same as in Papers I and II as were the criteria for spectral classification.

The UBV photometry was based on five plates in U, two plates in B and four plates in V. The emulsion types, filters and exposure times were the same as previously.

The relationship between the international system and the instrumental system gives the following equations:

$$V = V_{instr} + 0.15(B-V)_{instr} - 0.14$$

$$B-V = 0.98(B-V)_{instr} + 0.01$$

$$U-B = 0.99(U-B)_{instr} - 0.13(B-V)_{instr} + 0.15$$

The plates were measured with Konkoly Observatory' s Cuffey-type iris photometer. We used the photoelectric sequence of *Hoag (1961)*. The mean errors of the photographically determined colours were 0.10, 0.08, 0.07 in U,B and V, respectively.

INTERSTELLAR REDDENING

Adopting *Allen's(1973)* relation between the intrinsic colour index and spectral type we have derived the E(B-V), E(U-B) colour excesses using Allen's relation between the absolute magnitude and spectral type and computing the apparent distance modulus for each star. The stars were divided into seven groups according to their distance modulus: <7, 7-8, 8-9, 9-10, 10-11, 11-12 and >12 mag. and the mean distance modulus and the colour excesses for each subgroup were determined. The colour excesses determined in this way are plotted in Fig.1 as a function of the distance modulus. According to *Svolopoulos (1961)* the distance modulus of the NGC 7686 cluster is 8.6 mag. and the mean reddening equals 0.17 mag. which is in good agreement with our value. Adopting E(B-V) from Fig.1 and a ratio of total to selective absorption equal to 3.0, we have corrected the magnitudes for the absorption.

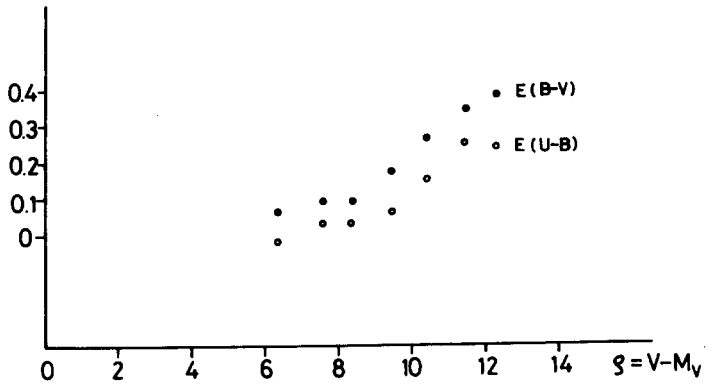

Fig.1 Colour excesses as functions of the apparent distance moduli of the stars.

SPACE DISTRIBUTION OF STARS

Preparing the input data for computation:

After removing the effect of interstellar absorption from the apparent magnitudes of the stars we determined the space densities of the stars in our sample by solving the basic convolution equation of stellar statistics

$$A(m) = \int_{-\infty}^{+\infty} D(y) f(m-y) dy$$

where A(m), D(y), f(m-y) are the number of stars in a (m,m+dm) magnitude interval, the probability density of distance moduli and the luminosity function of stars, respectively.

The stars were binned into subsamples to study the occasional dependence of space distribution on spectral type. The range of spectral types defining one subsample were chosen to ensure sufficient number of stars in each bin and taking into account the sharpness of classificational criteria. For this reason we have defined the five following bins: B8-A1, A2-A3, A4-A7, A8-F2, F3-F7. The distribution of stars against the V measured magnitude in the given subgroups is shown in Fig. 2a-f.

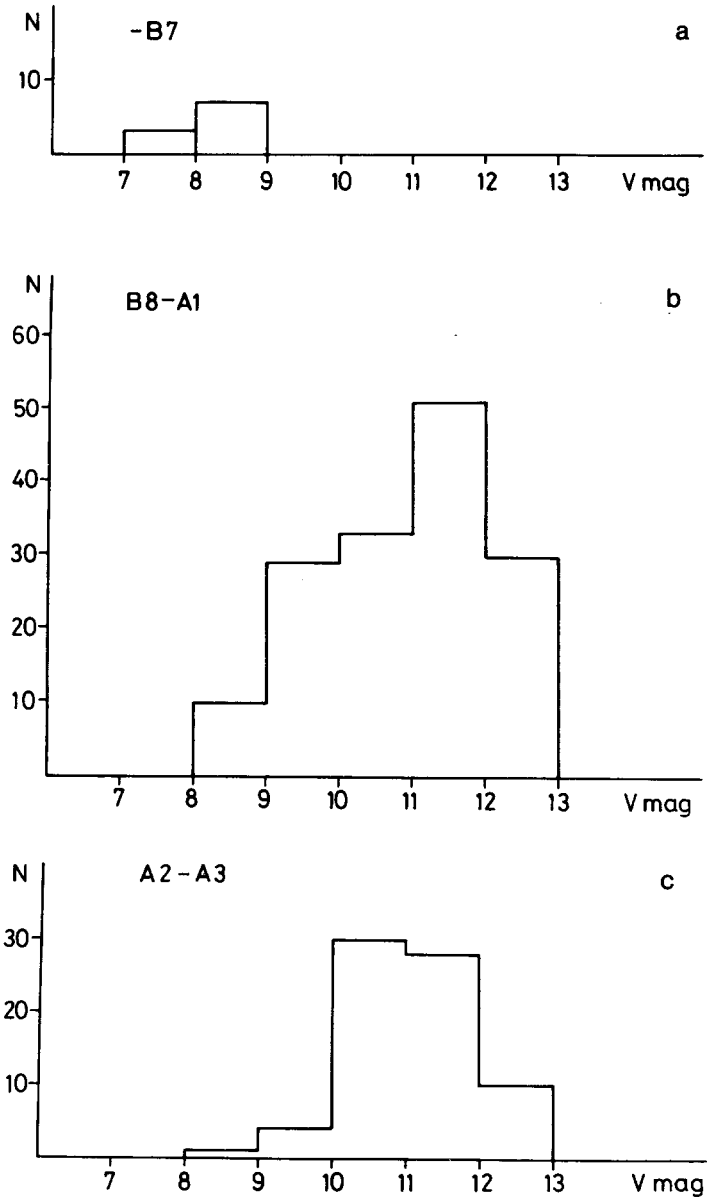

Fig.2a-c Distribution of stars against the V magnitude in different spectral ranges.

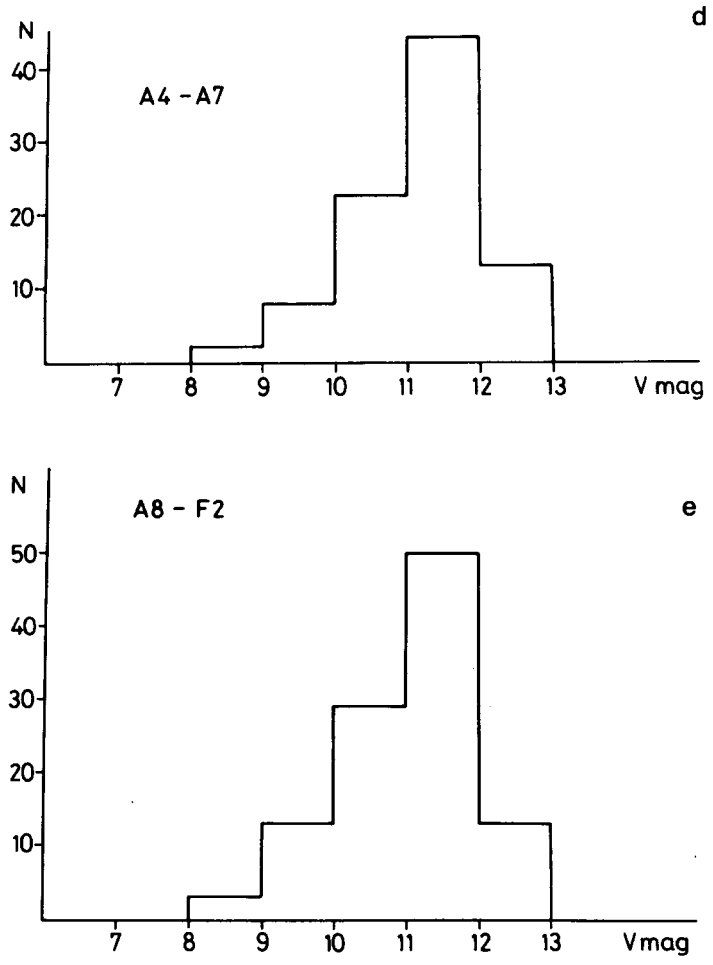

Fig.2d-e Distribution of stars against the V magnitude in different spectral ranges.

We assigned the mean absolute magnitude to each bin using the distributions of spectral types within them. The only exception was the B8-A1 group because of the lack of reliable classificational criteria of these stars on our small scale

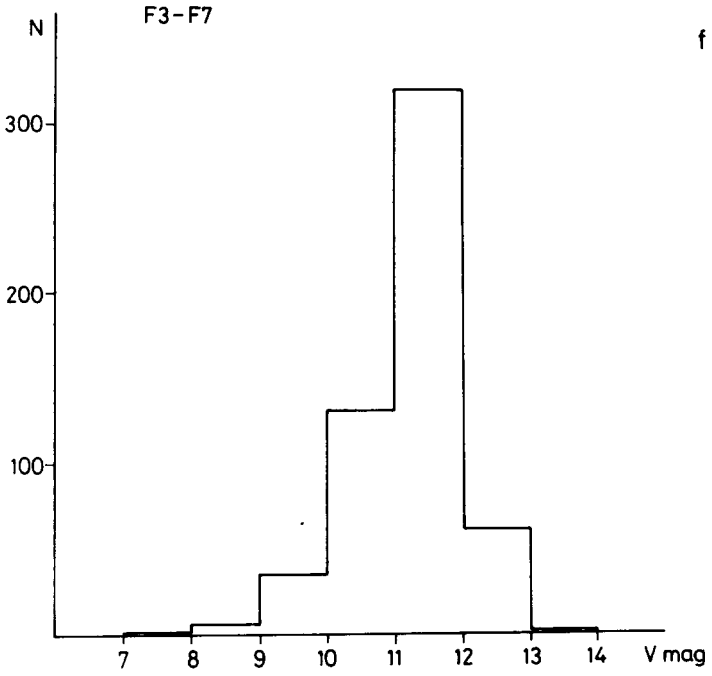

Fig.2f Distribution of stars against the V magnitude in F3-F7 spectral range.

spectra. To compute the mean absolute magnitudes of the corresponding subsamples we used the absolute magnitudes of *Allen (1973)* weighted with the distribution of spectral types observed.

To obtain the spatial densities in each spectral group defined above the convolution equation of stellar statistics was solved for them separately using the matrix method of *Dolan (1974)*. The luminosity function inside the spectral group was assumed to be Gaussian with a mean absolute magnitude equalling the mean absolute magnitude assigned to the subsample. The

standard deviation of the computed density values can be obtained from the formula yielding the densities.It is, however, obviously necessary to discuss in more detail the possible sources of bias inherent in this procedure.

The first source of bias is caused by the method itself. To solve the convolution equation we supposed that the form of the luminosity function is Gaussian, which is in fact true if one deals with a given spectral type (*McCuskey 1966*). In our case, however, we binned the data in a certain spectral range and used an average absolute magnitude to compute the densities. The distribution of absolute magnitudes could deviate significantly from the Gaussian depending on the distribution of spectral types inside the spectral range defined as one bin. We tried to eliminate this effect by grouping the stars into different spectral bins and comparing the densities obtained. No significant changes were observed in the case of A type stars. Eventually we binned the A type stars into groups A2-A3,A4-A7 and A8-F2. In these groups the ranges of absolute magnitudes are 0.2, 0.5 and 0.5, respectively. These variations are small compared with the about 1 magnitude standard deviations of absolute magnitudes for these spectral types. In groups B8-A1 and F3-F7, however, these figures are 1 and 0.8, respectively and if the distribution of spectral types has a significant skewness the distribution of absolute magnitudes cannot be described with one Gaussian in these subsamples and on solving the convolution equation assuming Gaussian distribution the bias could be inserted into the densities obtained.

Another possible source of bias comes from the uncertainties in the averaged absolute magnitude of stars assigned to the Gaussian-shaped luminosity function of a subsample. Its deviation from the true value causes changes in the distance scale and, consequently, in the spatial densities (0.5 mag. error in the absolute magnitudes results in a change of a factor of 2 in the densities). There is a significant difference between the calibrations made by different authors (e.g. for A0 stars *Alexander (1958)* reported 0.14, *Eggen (1962)* 0.85, *Perry (1969)* 0.71 *Hildich et al.* (1983) 1.2). Because we had no reliable

classificational criteria on our small scale spectra for B8-A1 stars we could not calculate the average absolute magnitude using the distribution of spectral types over this subsample. In view of this we assigned to this group an average absolute magnitude obtained from the spectral type distribution of stars near the Sun (data from *Allen(1973)*).

The third and probably the most serious bias in our determination of space densities was the truncation of our samples. The convolution model assumes that the measured quantity (in our case the apparent magnitude of stars) is a sum of two probability variates, i.e. the absolute magnitude and the distance modulus. Due to the limiting magnitude of the telescope utilized for the observations, we can observe only a part of the convolved sample for which the convolutional model holds exactly. If the truncated sample is used in our computations the result will be seriously biased because the sample does not fulfil the basic assumption of a convolution equation: the sample observed is generated by a convolution process. In the next paragraph we outline a way to overcome this difficulty and to separate a part of the computed spatial density curve that is only slightly biased.

Discussion of space densities:

Applying Dolan's method to the subsamples described in the previous paragraph we obtained the spatial density curves displayed in Fig.3a-e. A vertical dashed line indicates the estimated distance beyond which the densities are seriously biased due to the sample truncation. The estimation of this limit proceeded as follows: we visually inspected the distributions displayed in Fig.2; this revealed that all the subsamples contain only a few stars fainter than 12.5 magnitude. This value was adopted as the plate limit. We then computed the distance modulus using the plate limit and the absolute magnitude corresponding to the fainter edge of the spectral range of the subsample in question. Next we corrected this distance modulus for the absorption, and the distance obtained in this way was

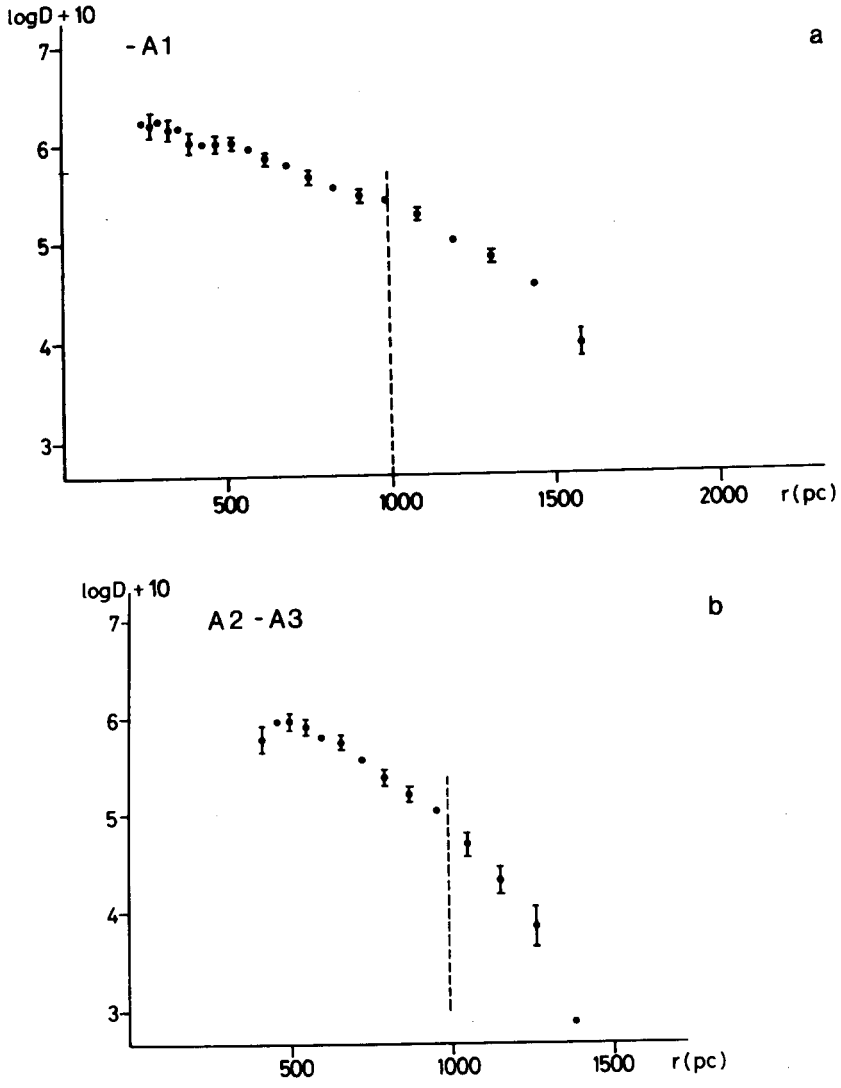

Fig.3a-b Space densities of stars in different spectral subgroups.
(The dashed line idicates the plate limit.)

adopted as the limit of the little-biased part of the density curves.

The most important remark to be made after inspecting the

density curves is to state that they do not display the inflexion feature described in the introductory paragraph of this paper. This inflexion feature was thought to be a consequence of the

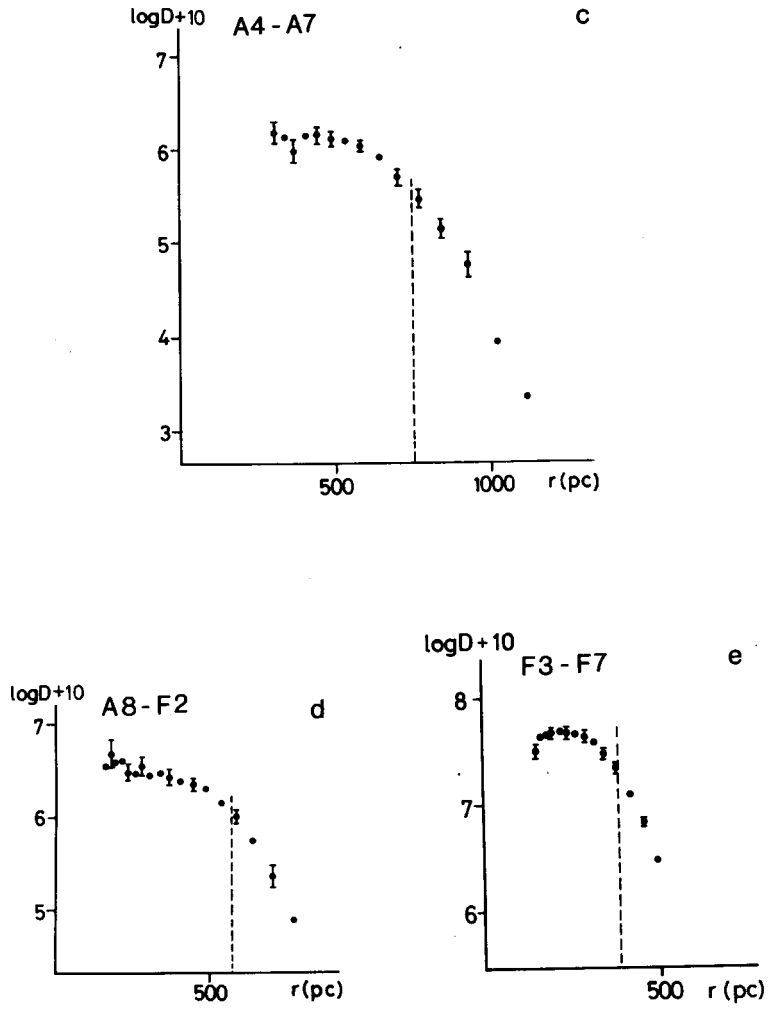

Fig.3c–e Space densities of stars in different spectral subgroups. (The dashed line indicates the plate limit.)

discontinuous star formation in the solar neighbourhood and of a subsequent dynamic evolution - as we pointed out in the introduction. *Oort(1932)*, *van Rhijn(1960)*, *Woolley and Stewart(1967)* accounted for the inflexion feature as being the superposition of subsystems having Gaussian (isothermal) velocity distribution of the velocity components perpendicular to the galactic plane but with different variances. The lack of inflexion on our curves may indicate that we could recognize only one isothermal component on the basis of our sample. This may be caused by the truncation due to the limiting magnitude of our observations. This means that the second isothermal component would have an influence beyond the bias-free part of the density curves. We shall discuss this assumption in more detail when comparing our empirical density curves with models.

Assuming that the density curves of A type stars represent essentially the different portions of the same density distribution we can construct a composite curve from the density curves of the A2-A3, A4-A7, A8-F2 subsamples. For constructing this we selected a common distance range on the little-biased parts of the density curves. This turned out to be at 500 pc. We normalized each curve by equalling the densities at this distance by shifting the curves vertically in the (log density; distance)

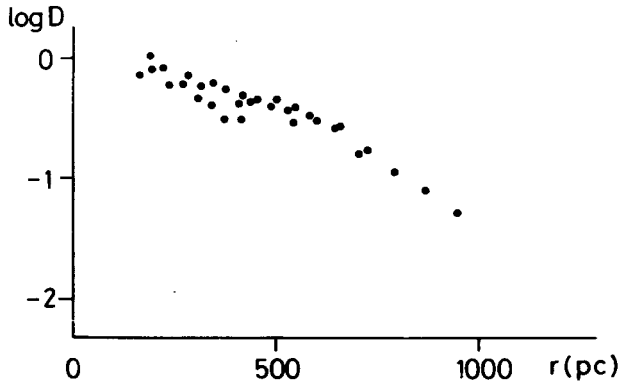

Fig.4 Composite space density curve of A type stars.

plane. The resulting curve obtained using this procedure is displayed in Fig.4.

We did not use the B8-A1 and F3-F7 stars in this procedure for different reasons. The density curve of B8-A1 is flatter than those of the A type stars in our sample. The flatness of the density curve may possibly be accounted for by assuming an about 0.5 magnitude systematic error in the absolute magnitude we used for determining the density distribution of this spectral range. We have already stressed above that the possible source of this systematic error was the lack of reliable classificational criteria on our small scale spectra in this spectral range. We have excluded the F3-F7 stars from these calculations because they did not have reliable density values near 500 pc.

Comparisons with models:

a. Exponential distribution

An exponential distribution is commonly used for describing the space distribution of stars perpendicular to the galactic plane. It was assumed also by *Bahcall and Soneira (1980)* for constructing their standard model of our Galaxy. It is so far the most detailed model of that type. Exponential models are represented by a straight line on the (log D, r) plane, where D is the spatial density and r is the distance in the line of sight. If our density plots of different spectral ranges are considered, it can be seen that the curves of B8-A1, A2-A3 and A8-F2 type stars can be represented by a sraight line in the 300-1000, 500-1000 and in the 200-500 pc distance range, respectively. Extrapolations of the densities to the galactic plane, however, yield in the case of A2-A3 stars about four-times higher values than observed whereas in A8-F2 range they are close to the values derived from the data of nearby stars *(Gliese,1969)*. With the A4-A7 stars the exponential fit is rather poor: the extrapolated density in the galactic plane, however, is close to the value of Gliese. Except for the A2-A3 group where the scale height is about 50 pc the scale heights are comparable

with those used by *Bahcall and Soneira (1980)*. The extrapolated density values in the galactic plane utilized by different models are listed in Table 1. The corresponding scale heights are summarized in Table 2. The composite density curve made up from the A-type stars (Fig.4) clearly shows a curvature and, correspondingly, an exponential model gives a poor fit to the data. The scale height of the best fitting exponential is about 70 pc in this case.

Table 1

Extrapolated densities in the galactic plane utilized by different models (log D(o)+10)

	A2-A3	A4-A7	A8-F2
Gliese catalog	6.25	6.66	6.89
Isothermal model	6.35	6.50	6.67
Exponential model	6.95	6.75	6.83

Table 2

Scale heights (pc) of the best fitting exponential models

	A2-A3	A4-A7	A8-F2
Exponential model	50	66	90
Standard model (Bahcall and Soneira 1980)	90	90	90

b. Camm's models

Camm (1950) studied self consistent solutions of the system consisting of a collisionless Boltzmann equation and the Poisson equation of the gravitational force field. He was looking for equilibrium configurations and found three particular solutions in the plane parallel case. His first solution corresponds to the isothermal case where the velocity dispersion is independent of the spatial coordinate. This result had actually already been found by *Spitzer(1942)*. The basic idea behind these calculations is that the stars obey the same distribution in the phase space independently of their spectral type. Comparing the distribution of A type stars with, for example, that of F type stars, this

assumption obviously does not hold. However, it is worth while to compare these models with our empirical density distributions. To facilitate comparison between the theoretical and empirical data we have displayed the empirical and model data on the (logD,logr) plane. The possible scale errors due to the systematic errors in absolute magnitudes appear as a shift along the log r axis. As to the isothermal model we shall return to its discussion later on in the context of the more advanced Bahcall model.

With regard to Camm's other two solutions, these models (Nos.II and III) were used more recently by *Hill, Hildich and Barnes (1979)* to explain the distributions of A and F type stars in the North Galactic Cap. The best fitting solution adopted by HHB was based on model No.II and it gives a reasonably good fit in the z < 200 pc distance range but deviates significantly from

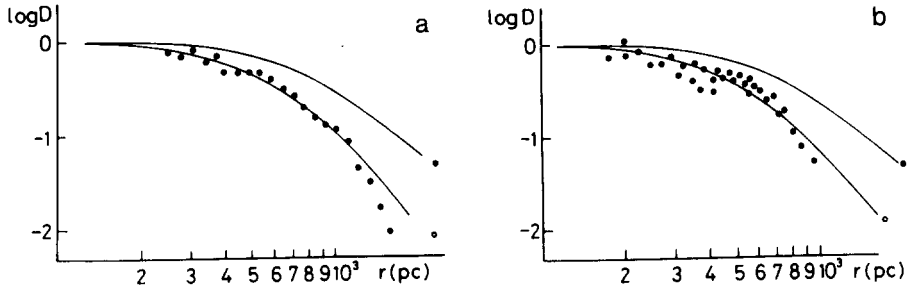

Fig.5 Comparison of space density distribution of B8-A1 stars (a) and of the composite density curve of A type stars (b) with the model of *Hill et al.(1979)*. (o HHB model for A type stars, ● HHB model for F type stars.)

the empirical plots of both the A and F type stars beyond this distance. Fig.5 shows a comparison between the B8-A1 stars (a) and our composite density curve of A type stars (b) with the HHB models after a suitable shift of the empirical curve in the log r direction to get the best fit with the model. As one can confirm from the figure the fit is satisfactory in case (a) and poorer in case (b) even in the distance range where the models give an excellent fit to the HHB data. As we shall discuss later

on, our data can be fitted quite well by an isothermal model and the discrepancy between our points and those of HHB might be accounted for by a systematic error inherent in deriving the space densities. One probable source of such a systematic error is the inaccurate deconvolution when determining the space densities from the magnitude data.

c. Bahcall's model

Bahcall attempted to find a self-consistent solution of the collisionless Boltzmann equation - Poisson equation pair assuming that the disc density can be written in the form of a sum of different isothermal components and a term representing the halo mass density. He made detailed calculations in the isothermal case. We have compared his model with our data in Fig.6 for

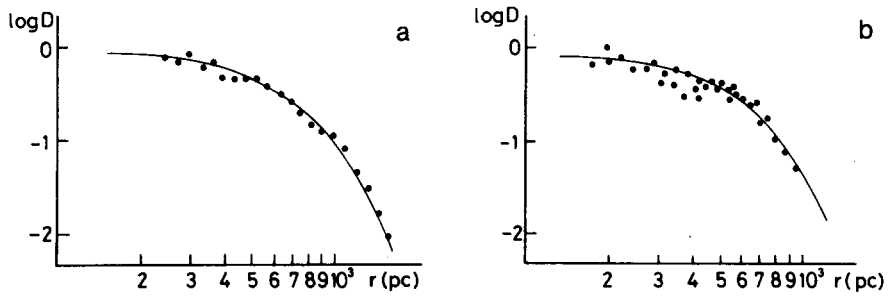

Fig.6 Comparisons of empirical space density curves with the *Bahcall*'s model (*1984*): a): B8-A1 b): composite density curve of A type stars.

B8-A1 stars (a) and for the composite distribution of our A type stars sample (b).

To get the closest fit we shifted the empirical plots along the log r axis corresponding to 1.45 and 1.8 times increase of the scales in the case of B8-A1 group and the composite curve

of A type stars, respectively. The scale differences might be accounted for not by the systematic errors of absolute magnitudes we used to derive the corresponding space densities but rather by the differences in the velocity dispersions assigned to the best fitting isothermal distribution for A and F type stars. The latter was used to fit the Bahcall model. The 1.24 times larger scale of B8-A1 stars in relation to the A type spectral group can be explained by a 0.5 magnitude systematic error in absolute magnitudes. The possibility of such an error was mentioned in paragraph 3.2 when we discussed the space densities of the sample stars.

Summarizing what has been said, our view is that the space distribution of B8-A1 and A type stars in our sample can be represented very well by Bahcall's isothermal model after appropriate scale transformation.

d. Two component model of Woolley and Stewart

Woolley and Stewart (1967) worked out a model superposing two isothermal components having a ratio of the velocity

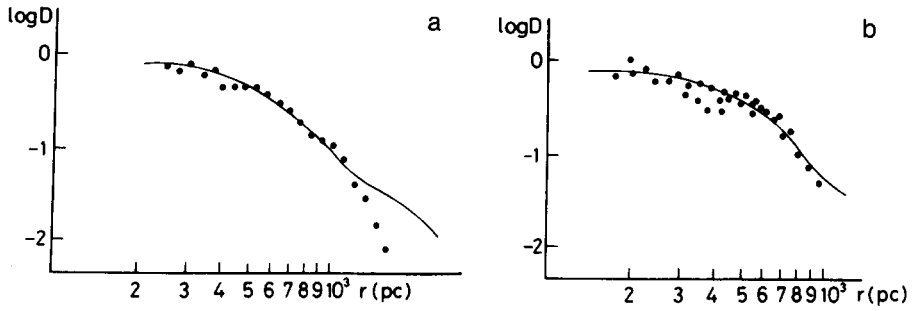

Fig.7 Fitting the empirical space densities by the model of *Woolley and Stewart (1967)*. a): B8-A1 stars b): A type stars. The model tends to deviate from the empirical curve beyond the limit of completeness of the empirical data. (We achieved the best fit with the WS model by shifting our experimental density plots by 0.04 and 0.13 along the log r direction for a) and b), respectively.)

dispersions of about 1:2. The aim of their model was to explain the inflexion feature inherent on the space density curve of A type stars perpendicular to the galactic plane. We have achieved the best fitting with the WS model by shifting our experimental density plots in the (log D,log r) plane by 0.04 and 0.13 along the log r direction in the case of B8-A1 and A type stars, respectively (see Fig. 7a and b). Below the inflexion the space distribution is dominated by one isothermal component and this part coincides well with the plots derived from our observations. The deviation from a simple isothermal model becomes significant beyond the limit of completeness of our sample so this limit does not enable us to study the possible presence of a secondary isothermal component in our data.

Mass density in the solar neighbourhood:

The total mass density could be determined knowing the gravitational potential by using the Poisson equation (see e.g. *Oort 1965*). In the case of isothermal distribution the logarithm of space density is proportional to the gravitational potential if we consider the plane parallel case:

$$\log D(z) - \log D(0) = -\frac{\varphi(z)}{\sigma_w^2}$$

where $D(z), \varphi(z), \sigma_w^2$ are the spatial density, gravitational potential and variance of velocities perpendicular to the galactic plane, respectively. Expanding $\varphi(z)$ into Taylor series and supposing that $\varphi(z)$ is symmetric to the galactic plane we have:

$$\varphi(z) \approx \varphi(0) + \frac{\varphi''(0)}{2} z^2 + \ldots$$

The log density could, therefore, be fitted by a simple parabola if z is sufficiently small for the higher order terms in this expansion to be neglected. Since the total mass density is connected with the potential by the Poisson equation the coefficient of the second order term in the expression of the log

density is given by

$$a = \frac{2\pi G\rho(0)}{\sigma_w^2}$$

where G, $\rho(0)$ are the gravitational constant and the total mass density in the plane of the Galaxy, respectively. Comparing our density curves with a suitably chosen parabola we can get an excellent fit to our B8-A1 and composite A type stars density curve (see Fig.8). We may conclude, therefore, that the parabola approximation is satisfactory in the $z<200$ pc range. Adopting $\sigma_w = 7.3\pm2$ km/sec (*Hill et al. 1979*) we get $\rho(0)=0.104\ M_\odot/pc^3$ and $\rho(0)=0.159\ M_\odot/pc^3$ in the case of B8-A1 and A type stars, respectively. Nevertheless, it is necessary to remark that the mass density derived from the B8-A1 sample is probably underestimated because of the possible scaling error of 1.24 (as pointed out in 3.2 paragraph). The total mass density of matter observed in the solar neighbourhood has an estimated value of $\rho(0)=0.108\ M_\odot/pc^3$ (*Hill et al.1979*). Taking into account the 2 km/sec standard deviation of velocity dispersion and computing $\rho(0)$ with $\sigma_w=5.3$ km/sec instead of 7.3 km/sec we get a mass density of $\rho(0)=0.084\ M_\odot/pc^3$. Thus the observed mass density is within the confidence interval of the derived mass density and there is no significant difference between the observed and

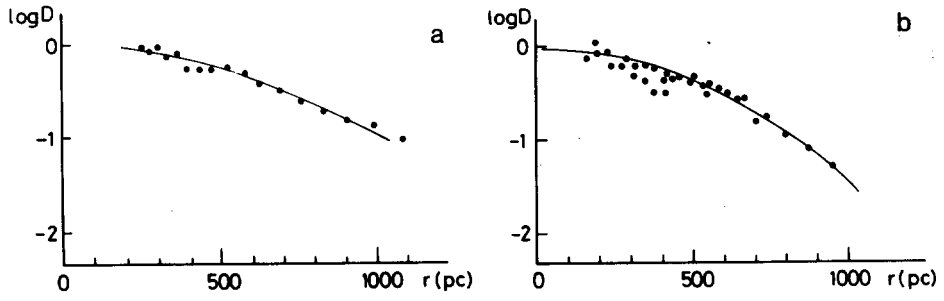

Fig.8 Parabola approximation of the empirical density curves: a): B8-A1 stars b): A type stars. The estimated values of the total local galactic mass density are 0.105 $M_\odot/pc^3$ and 0.159 $M_\odot/pc^3$ for a) and b), respectively.

computed local mass density. There are several papers, however, pointing towards the value of $\rho(0)=0.15\ M_{\odot}/pc^3$ thereby indicating the presence of a considerable amount of unseen matter near the Sun (*Oort 1965, Hill et al. 1979, Bahcall 1984*). Moreover the applicability of A type stars for determining the local mass density is also criticized (*King 1983, Bahcall 1984*) on the basis that they do not display a fully relaxed subsystem. We think, however, that the excellent fit given by a simple isothermal model to our empirical density curves of A type stars in our sample gives some support for the reliability of the procedure we applied to obtain the total mass density in our galactic neighbourhood.

CONCLUSIONS

We have studied the space distribution of interstellar matter and stars earlier than F7 in a 19.5 sq. degrees field centred on NGC 7686.

Using the spectral and colour data, we derived the interstellar absorption as $A_V=1.2$ mag.

After removing the effect of absorption we computed the spatial densities in the subsamples given by the spectral ranges of B8-A1, A2-A3, A4-A7, A8-F2, F3-F7. Normalizing the densities to the density at 500 pc we made a composite density curve for the A type stars.

The most significant remark to be made after inspecting the shape of the density curves obtained is that these curves do not display an inflexion indicating the possible presence of kinematically different subsystems as was found in our previous works and in the references listed therein.

We have compared our density curves with an exponential density distribution, with Camm's models, with Bahcall's model and with the two component model of Woolley and Stewart. We have found that the best fit is given by an isothermal model. Comparison with the WS model (yielding an inflexion by superposing two kinematically different isothermal components) indicated that the inflexion lies beyond the limit of

completeness of our sample. If the magnitude limit were to be extended by at least 1 mag. this could clear up whether this is in fact the case.

The best fitting isothermal model enabled us to compute the total mass density of matter near the Sun. We have obtained a value of 0.104 $M_\odot/pc^3$ for the B8-A1 group, and 0.159 $M_\odot/pc^3$ for the A type stars in our sample. The density obtained from the B8-A1 stars is probably underestimated because of a possible scale error of a factor of 1.24 due to the absolute magnitudes we used for this spectral group. Taking into account the uncertainties of velocity dispersions used in our computations the 0.108 $M_\odot/pc^3$ observed mass density does not differ on the one sigma level from the computed one. Results of other authors, however, point to a value of about 0.15 $M_\odot/pc^3$ indicating the presence of a considerable amount of dark matter near the Sun.

ACKNOWLEDGEMENTS

We are indebted to Dr. B. Szeidl for his advice on eliminating systematic errors from our colour data. The assistance of Mrs.I. Kalman in measuring the photographic UBV data is also acknowledged.

Budapest, December 16, 1985.

REFERENCES

Alexander, J.B., 1958, MNRAS, 118. 161.

Allen, C.W., 1973, Astrophysical Quantities 3rd.ed., Athlona Press London.

Bahcall, J.N., Soneira, R.M., 1980, Ap.J.Suppl.44.77.

Bahcall, J.N., 1984, Ap.J.276.169.

Balazs, L.G., 1975, Mitt. Sternwarte Ung.Ak.Wiss.No.68.(Paper I)

Balazs, L.G., 1977, The Cosmogonical Significance of the z Distribution of Stars in "Chemical and Dynamical Evolution of our Galaxy" IAU Coll. No.45.p.271.

Balazs, L.G., 1984, Statistics of A-Type Stars as Possible Indicator of Star Formation in "Astronomy with Schmidt-Type Telescopes" ed. M.Capaccioli, D.Reidel Publ.Co.p.269.

Camm, G.L., 1950, MNRAS 110.305.

Dolan, J.F., 1974,Astron. and Astrophys.35.5.

Eggen, O.J., 1962, R.Obs.Bull. No.42.

Gliese, W., 1969, Catalog of Nearby Stars (Veröff.Astr. Rechen-Inst. Heidelberg, Nr.22.)

Hildich, R.W., Hill, G., Barnes, J.V., 1983, MNRAS 204.241.

Hill, G. Hildich, R.W., Barnes, J.V., 1979, MNRAS 186.813.

Hoag, A.A., 1961, Publ.USNav.Obs. No.17.347.

King, I.R., 1983, On the Analysis of Motions Perpendicular to the Galactic Plane in "Kinematics, Dynamics and Structure of the Milky Way" ed. W.L.H. Shuter, D. Reidel Publ.Co.p.53.

Lacey, S.C., 1984, MNRAS 208.687.

McCuskey, S.W., 1966, Vistas in Astron. 7.141.

Oort, J.H., 1932, BAN 6.249.

Oort, J.H., 1965, Stellar Dynamics in "Galactic Structure", ed. A.Blauw and M.Schmidt, Univ. Chicago Press, p.455.

Palous, J., Piskunov, A.E., 1985, Astron. and Astrophys. 118.306.

Paparo, M., Balazs, L.G., 1982, Mitt. Sternwarte Ung.Ak.Wiss. No.82. (Paper II)

Perry, C.L., 1969, Astron.J. 74.139.

Spitzer, L., 1942, Ap.J. 95.239.

Spitzer, L., Schwarzschild, M., 1953, Ap.J. 118.306.

Svolopoulos, S.N., 1961, Ap.J. 134.612.
van Rhijn, P.J., 1960, Publ. Kapteyn Astr.Lab. Groningen No.61.
Villumsen, J.V., 1984, preprint (submitted to the Ap.J.)
Wielen, R., 1977, Astron. and Astrophys. 60.263.
Wielen, R., Fuchs, B., 1983, Velocity Distribution of Stars and Relaxation in the Galactic Disk in "Kinematics and Structure of the Milky Way" ed. W.L.H. Shuter, D. Reidel Publ.Co. p.81.
Woolley, R., Stewart, J.M., 1967, MNRAS 136.329.

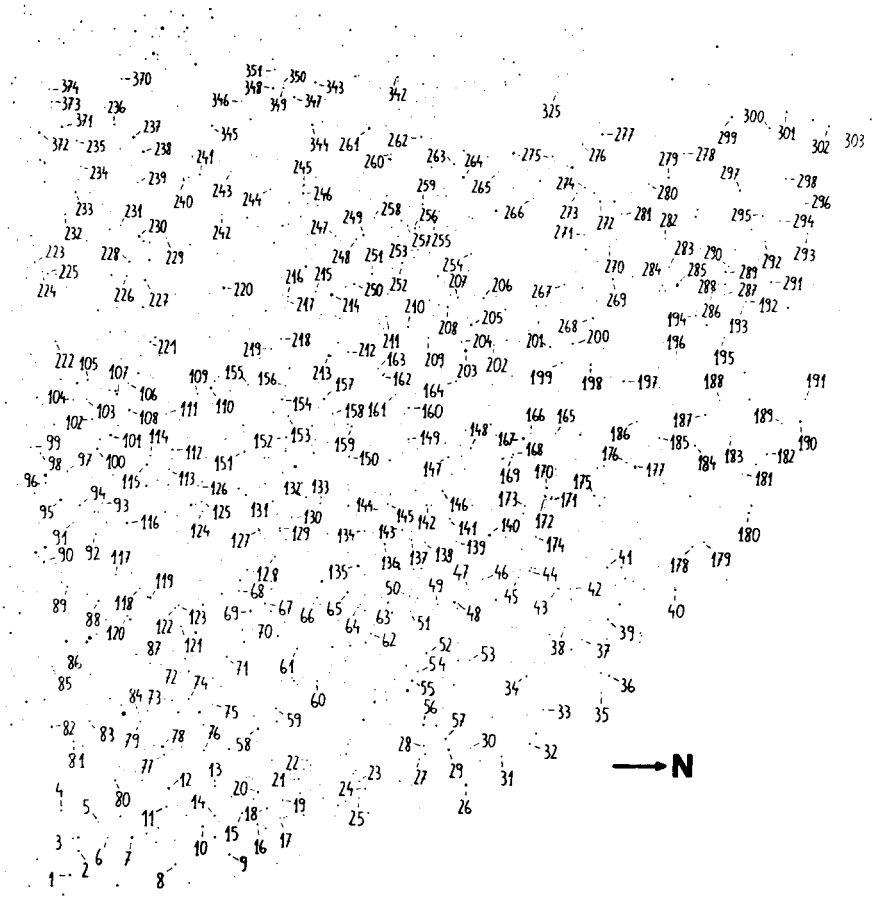

Finding chart of the survey stars

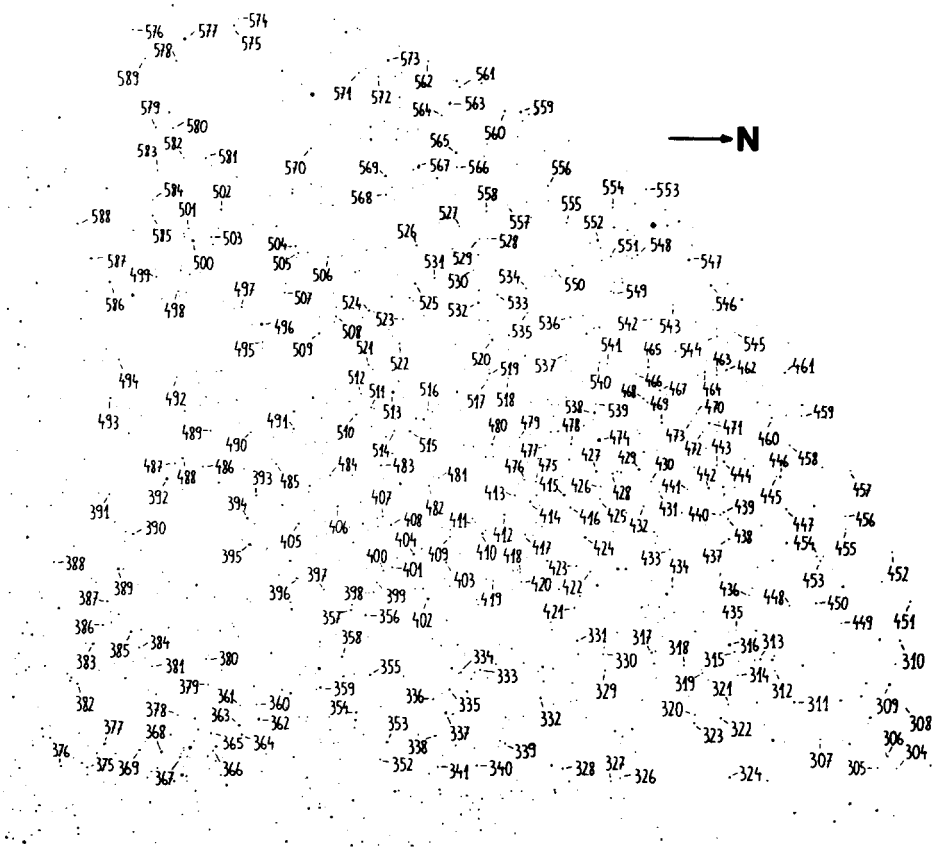

Finding chart of the survey stars

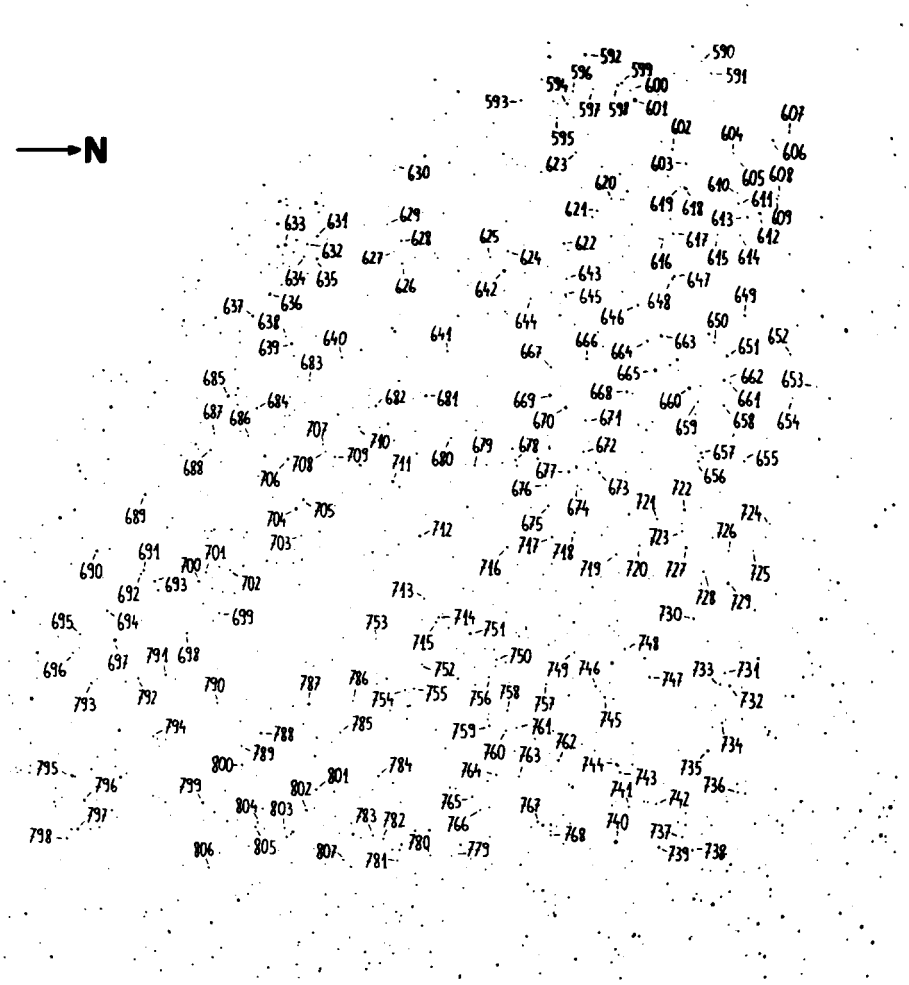

Finding chart of the survey stars

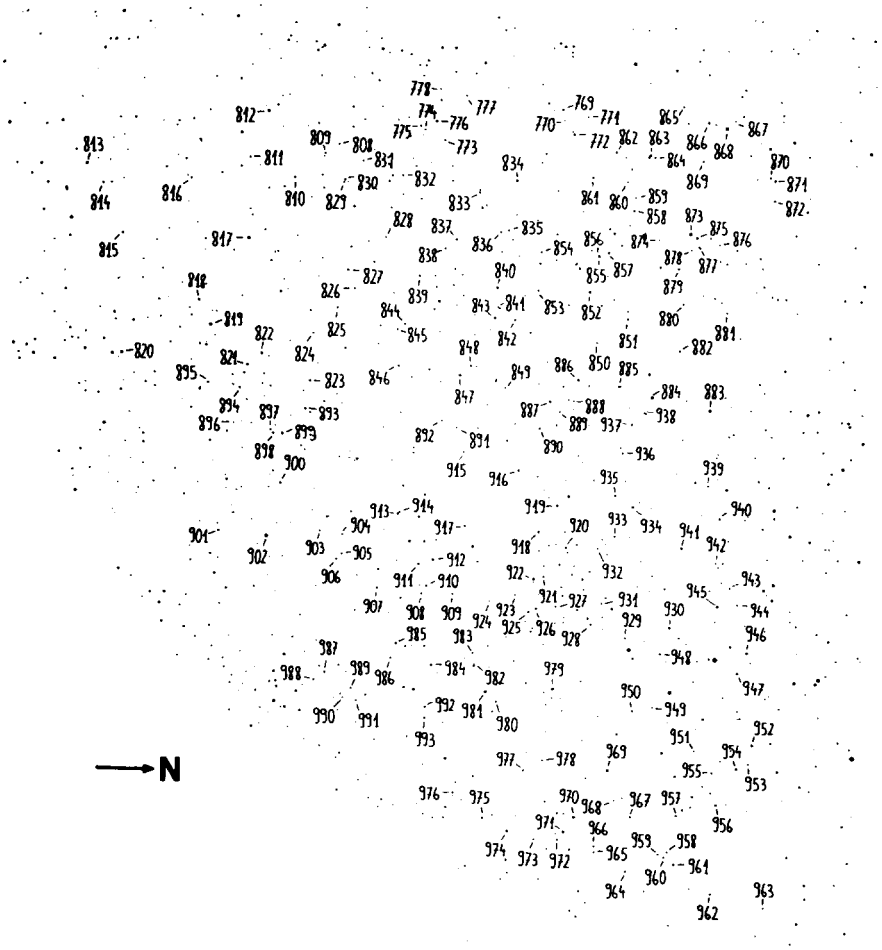

Finding chart of the survey stars

TABLE

Spectra and UBV data of survey stars

No.	Sp.	V	B-V	U-B	No.	Sp.	V	B-V	U-B
1	A9	9.58	0.51	0.19	51	A6	12.91	0.40	0.27
2	F7	10.39	0.84	0.16	52	F7	10.45	0.62	0.10
3	A2	10.77	0.34	-0.06	53	A0	12.47	0.36	0.03
4	A9	11.29	0.38	0.24	54	F6	11.63	0.47	0.11
5	A8	12.43	0.66	-0.02	55	F6	10.52	0.71	0.11
6	A2	12.12	0.37	0.13	56	F7	10.40	0.72	0.03
7	A0	9.38	0.30	-0.06	57	A2	10.24	0.28	0.30
8	A1	11.18	0.40	0.23	58	A2	10.00	0.30	0.18
9	F4	10.91	0.47	0.07	59	F7	11.09	0.50	0.12
10	F2	10.49	0.52	0.11	60	F6	11.57	0.58	0.18
11	F7	11.29	0.64	0.20	61	A1	11.58	0.26	0.12
12	F7	9.91	0.67	-0.02	62	F7	12.04	0.80	0.03
13	A7	11.75	0.51	0.33	63	F6	11.54	0.76	0.08
14	F7	11.16	0.73	0.00	64	B8	12.38	0.37	0.28
15	F0	11.80	0.60	-0.05	65	A1	11.15	0.13	-0.09
16	F7	11.28	0.79	0.09	66	A0	11.83	0.30	0.04
17	F7	11.84	0.90	0.13	67	F7	10.95	0.72	0.14
18	F7	11.42	0.69	-0.19	68	F7	11.85	0.64	0.19
19	F5	11.82	0.65	0.12	69	A1	9.98	0.17	0.13
20	F7	10.51	0.79	-0.11	70	F7	12.14	0.75	-0.04
21	F2	11.78	0.59	0.05	71	F5	11.37	0.53	0.14
22	A4	11.77	0.51	0.27	72	F7	11.08	0.68	0.16
23	A4	12.31	0.53	0.23	73	F0:	11.56	0.57	0.04
24	F7	11.59	0.81	0.05	74	F7	11.21	0.56	0.09
25	A1	12.22	0.56	0.12	75	A3	12.16	0.49	0.20
26	A1	8.97	0.32	0.19	76	F6	11.36	0.57	0.13
27	A7	11.77	0.59	0.00	77	F7	11.91	0.72	0.10
28	F7	11.15	0.92	0.25	78	A5	9.52	0.33	0.32
29	A2	10.60	0.31	0.08	79	F3	11.71	0.49	0.22
30	F7	11.92	0.77	0.01	80	F7	11.05	0.56	0.21
31	A2	11.22	0.59	0.06	81	F0	10.92	0.35	0.25
32	A5	10.82	0.46	0.18	82	F3	10.15	0.34	0.19
33	A4	11.76	0.48	0.32	83	F5	11.76	0.42	0.11
34	F2	10.84	0.49	0.22	84	F3	11.75	0.90	0.28
35	F6	11.26	0.61	0.22	85	F1	11.92	0.78	0.09
36	A5	10.83	0.51	0.21	86	A5	8.65	0.20	0.23
37	F7	11.74	0.61	0.26	87	F6	11.44	0.59	0.01
38	A0	11.58	0.36	0.19	88	F4	10.89	0.49	0.14
39	F0	11.32	0.40	0.33	89	F7	11.68	0.62	0.18
40	A3	10.46	0.32	0.45	90	A0	10.26	0.18	-0.04
41	A1	11.35	0.37	0.26	91	F4	12.22	0.66	-0.02
42	A5	11.86	0.38	0.37	92	F6	11.89	0.62	-0.08
43	F7	10.10	0.48	0.21	93	F7	12.54	0.44	0.05
44	A1	11.36	0.41	0.24	94	F6	10.67	0.61	-0.03
45	A0	12.26	0.36	0.19	95	A6	8.99	0.34	0.21
46	F7	11.17	0.64	0.15	96	F7	11.09	0.70	-0.12
47	A8	12.12	0.49	0.20	97	F7	11.72	0.67	-0.05
48	F5	11.04	0.47	0.27	98	F7	11.72	0.66	-0.09
49	F6	11.63	0.52	0.14	99	F7	11.68	0.71	-0.09
50	A3	12.09	0.29	0.36	100	F5	10.38	0.56	0.07

TABLE

No.	Sp.	V	B-V	U-B	No.	Sp.	V	B-V	U-B
101	A7	9.40	0.34	0.09	151	F6	10.75	0.50	-0.02
102	F7	11.86	0.75	-0.09	152	F6	10.91	0.66	-0.10
103	A3	11.79	0.42	0.17	153	F5	11.33	0.55	0.17
104	F7	12.02	0.60	-0.07	154	A2	11.01	0.20	0.03
105	F4	10.86	0.45	0.05	155	F0	12.27	0.30	0.12
106	A0	12.37	0.46	-0.02	156	F5	11.43	0.56	0.09
107	A1	10.52	0.19	-0.05	157	A5	10.25	0.38	0.11
108	F1:	10.49	0.34	0.16	158	F0	11.86	0.55	0.16
109	F7	11.45	0.78	0.02	159	A1	11.12	0.23	-0.09
110	A0	9.14	0.11	-0.04	160	F6	10.29	0.64	-0.17
111	A5:	11.86	0.38	0.32	161	F7	11.68	0.65	0.03
112	F6	10.34	0.54	-0.01	162	F5	11.63	0.67	-0.03
113	F4	11.54	0.64	-0.16	163	F7	11.67	0.69	-0.11
114	A1	11.61	0.30	0.20	164	F2:	11.11	0.52	0.15
115	A1	10.29	0.12	0.02	165	F7	11.68	0.78	0.05
116	A2	9.59	0.31	0.14	166	F7	12.06	0.64	0.00
117	F7	12.01	0.54	0.05	167	B8	8.45	0.04	-0.11
118	A7	12.37	0.34	0.06	168	F7	10.90	0.69	0.09
119	F6	9.94	0.56	0.04	169	A0	11.59	0.26	0.17
120	A0	11.68	0.30	0.12	170	F6	9.43	0.64	-0.06
121	A0	11.87	0.24	0.01	171	F7	11.00	0.53	0.12
122	F7	11.05	0.66	0.00	172	F5	10.96	0.63	0.05
123	F7	11.69	0.63	-0.26	173	F7	11.27	0.72	0.15
124	F5	11.91	0.61	-0.03	174	A1	11.42	0.44	0.24
125	A0	12.07	0.40	0.14	175	F7	10.90	0.68	0.28
126	A0	12.74	0.16	-0.42	176	A4:	11.39	0.26	0.25
127	F0:	10.43	0.52	-0.01	177	F1	10.29	0.52	0.57
128	A1	11.90	0.32	-0.09	178	F7	10.94	0.63	0.31
129	A6:	11.12	0.46	0.07	179	A8:	11.06	0.51	0.45
130	A0	12.34	0.25	0.09	180	A1	10.24	0.64	0.09
131	F6	11.57	0.57	-0.09	181	F7	11.06	0.78	0.24
132	F6	11.67	0.73	-0.04	182	A0	12.01	0.36	0.79
133	F7	11.59	0.71	-0.17	183	F7	11.26	1.15	-0.28
134	F6	11.52	0.68	0.01	184	A7	10.30	0.59	0.34
135	A0	8.86	0.01	-0.12	185	A1	11.09	0.42	0.61
136	A0	11.10	0.39	-0.04	186	F7	11.45	0.96	-0.07
137	A4	12.06	0.41	0.18	187	F1	9.51	0.57	0.33
138	F7	11.92	0.70	-0.03	188	A3	11.31	0.72	0.29
139	A6	12.09	0.41	0.18	189	F7	10.39	0.74	0.34
140	B9	9.28	0.04	-0.16	190	B7	8.83	0.24	0.04
141	F0	11.79	0.60	-0.01	191	F7	10.91	1.09	0.15
142	F7	11.53	0.71	-0.07	192	F3	11.30	0.71	0.20
143	A2	11.69	0.30	0.26	193	F3	11.25	0.81	0.19
144	A8	11.70	0.45	0.09	194	F4	10.68	0.80	-0.05
145	F7	11.48	0.79	0.26	195	A1	11.20	0.61	0.22
146	F4	11.39	0.60	-0.06	196	A0	11.93	0.47	0.24
147	F7	10.83	0.90	0.31	197	A3	10.24	0.31	0.17
148	F6	10.60	0.57	0.08	198	A3	10.52	0.26	0.26
149	A4	11.30	0.32	0.17	199	F6	10.88	0.61	0.11
150	F4	11.05	0.48	0.04	200	A3	10.32	0.34	0.09

TABLE

No.	Sp.	V	B-V	U-B	No.	Sp.	V	B-V	U-B
201	F4	10.18	0.68	-0.06	251	F7	10.55	0.71	0.01
202	A0	11.59	0.56	0.15	252	F6	10.45	0.61	-0.10
203	B6	7.93	-0.05	-0.23	253	F5	11.84	0.88	-0.02
204	F0	11.31	0.59	0.11	254	F2	11.65	0.65	0.11
205	A1	9.83	0.28	0.11	255	F4	11.17	0.71	0.32
206	A2	10.86	0.32	0.03	256	F7	11.21	0.75	0.12
207	F1:	11.41	0.51	-0.04	257	F7	11.51	0.71	-0.10
208	F7	10.40	0.88	-0.08	258	A3	12.16	0.36	0.06
209	A5	11.80	0.45	0.05	259	A2	11.07	0.43	0.13
210	A3	11.12	0.24	0.21	260	F7	11.53	0.62	0.01
211	F3	11.63	0.37	0.09	261	F5	9.28	0.46	-0.08
212	A2	11.88	0.55	-0.02	262	F5	10.94	0.55	-0.04
213	A1	10.48	0.24	-0.01	263	F0	10.94	0.41	0.07
214	B7	8.39	0.05	-0.06	264	A5	9.29	0.31	0.14
215	F5	10.87	0.57	0.18	265	A0	12.56	0.09	-0.06
216	F7:	11.79	0.72	0.02	266	A0	12.32	0.25	-0.12
217	F6	11.87	0.71	0.02	267	F7	10.87	0.73	0.03
218	F5	11.61	0.49	0.08	268	F7	11.47	0.60	0.01
219	A8:	11.48	0.55	-0.16	269	A0	10.79	0.26	-0.08
220	A0	8.66	0.17	-0.02	270	F4	11.49	0.74	-0.04
221	F7	10.64	0.67	-0.15	271	A8	11.91	0.45	0.08
222	F0:	10.54	0.45	0.00	272	F7	11.19	0.25	0.42
223	F7	11.49	0.65	-0.03	273	F4	11.97	0.66	-0.10
224	F7	12.01	0.57	-0.12	274	F7	11.48	0.67	-0.17
225	F6	11.35	0.52	0.08	275	F5	11.09	0.54	0.13
226	F3	11.01	0.56	-0.08	276	F7	11.22	0.62	-0.09
227	F5	10.14	0.58	-0.15	277	A6	10.72	0.28	0.11
228	A2	10.25	0.41	0.14	278	A9	11.26	0.53	0.14
229	A1	12.33	0.33	0.05	279	A0	10.31	0.52	-0.03
230	A2	9.40	0.32	0.13	280	A2	11.32	0.44	0.16
231	F7	11.41	0.78	-0.06	281	F7	11.57	0.71	-0.19
232	A6:	11.37	0.38	0.08	282	F7	11.41	0.74	-0.10
233	F5	10.68	0.48	-0.08	283	F7	11.25	0.59	0.13
234	F7	12.61	0.64	0.00	284	A7	11.11	0.48	0.21
235	F5	11.40	0.46	0.14	285	F6	10.49	0.68	-0.09
236	F7	10.56	0.63	0.01	286	A3	11.59	0.27	0.15
237	F2	8.95	0.47	0.18	287	A0	11.98	0.35	0.26
238	A1	9.46	0.12	-0.11	288	F7	10.55	0.78	0.13
239	A1	11.81	0.31	0.04	289	A1	10.53	0.54	0.18
240	A4	11.26	0.35	0.15	290	F7	11.18	0.78	0.20
241	F7	10.61	0.75	0.08	291	A0	10.27	0.41	0.20
242	F7	11.74	0.63	0.05	292	A2	11.06	0.66	0.06
243	F7	11.70	1.04	-0.05	293	F7	9.95	0.76	0.24
244	F7	10.77	0.65	-0.07	294	F6	10.95	0.90	0.04
245	A1	11.56	0.16	0.18	295	F7	10.18	1.01	0.02
246	A1	10.44	0.19	0.04	296	F7	10.68	0.79	0.27
247	F7	11.60	0.72	-0.02	297	A0	9.94	0.52	0.02
248	A2	11.84	0.35	0.08	298	A2	10.48	0.46	0.38
249	F5	10.28	0.51	0.28	299	A3	10.03	0.64	-0.06
250	A6	10.22	0.32	0.19	300	A2:	10.58	0.42	0.34

TABLE

No.	Sp.	V	B-V	U-B	No.	Sp.	V	B-V	U-B
301	F5	8.87	0.70	0.24	351	F7	11.95	0.40	0.10
302	A3	10.61	0.37	0.59	352	F7	11.72	0.60	-0.01
303	F7	10.47	0.51	0.49	353	F5	10.31	0.44	0.12
304	F7	11.16	0.58	0.69	354	F5	10.72	0.52	-0.09
305	F7	11.47	0.76	0.45	355	A7	11.08	0.26	0.09
306	F7	11.18	0.55	0.49	356	A6	10.98	0.26	0.19
307	F7	11.38	0.87	-0.11	357	F6	11.17	0.42	0.14
308	A0	11.32	-0.09	-0.14	358	F7	11.26	0.55	0.09
309	A0	8.91	0.08	0.39	359	F7	10.11	0.60	0.05
310	F6	10.12	0.41	0.57	360	F7	11.89	0.62	-0.22
311	F7	9.82	0.82	0.04	361	F7	12.23	0.82	-0.05
312	F0	11.39	0.55	0.20	362	B9	9.53	0.06	-0.04
313	F6	10.45	0.67	-0.13	363	A0	9.93	0.26	0.03
314	F7	11.41	0.65	0.12	364	A0	10.35	0.15	0.29
315	A8:	10.83	0.38	0.08	365	A8	11.18	0.38	0.10
316	B8	8.62	0.08	-0.13	366	F7	11.65	0.40	0.02
317	A1	11.01	0.28	0.03	367	F5	11.56	0.55	0.09
318	F6	11.22	0.62	0.17	368	F6	10.30	0.43	0.06
319	F7	11.97	0.69	-0.06	369	F7	11.29	0.43	0.16
320	F7	11.36	0.64	-0.28	370	A6	11.48	0.49	0.10
321	F3	11.46	0.57	0.08	371	A7	9.95	0.29	0.05
322	F6	10.51	0.60	-0.04	372	A2	10.21	0.48	-0.02
323	A2	10.77	0.48	0.08	373	A5	11.73	0.30	0.11
324	A0	10.29	0.34	-0.21	374	A0	12.58	0.30	0.12
325	A0	12.13	0.18	0.02	375	F4	11.98	0.44	0.01
326	F7	11.86	0.80	-0.08	376	A7	12.00	0.42	0.14
327	A4	12.06	0.44	0.15	377	A4	11.52	0.23	0.27
328	F7	10.81	0.58	0.05	378	A3:	12.52	0.18	-0.01
329	A4	11.03	0.34	0.04	379	A1	12.25	0.34	0.06
330	F2	11.61	0.57	0.02	380	F7	12.13	0.49	-0.20
331	F4	10.91	0.40	0.00	381	F7	12.19	0.65	0.37
332	F0	10.49	0.36	0.11	382	F7	11.27	0.58	-0.17
333	F7	11.44	0.46	0.00	383	A2	10.27	0.36	-0.06
334	F7	11.27	0.64	-0.18	384	F6	12.02	0.50	-0.07
335	A0	11.01	0.32	0.04	385	F6	10.07	0.54	0.01
336	F7	11.43	0.54	0.06	386	F6	11.41	0.50	0.10
337	B6	8.75	-0.06	-0.25	387	F4	10.74	0.49	0.09
338	F7	11.23	0.47	0.14	388	F5	11.14	0.45	0.17
339	F7	11.49	0.63	0.11	389	F5	9.10	0.39	-0.17
340	A0	11.39	0.25	0.10	390	A4:	10.46	0.10	0.15
341	F7	11.36	0.51	0.05	391	A5	11.77	0.16	0.17
342	F7	10.62	0.57	0.00	392	A0	9.17	-0.10	-0.20
343	A9	10.44	0.41	0.06	393	F7	11.31	0.49	-0.01
344	F7	9.83	0.74	0.00	394	F7	9.54	0.55	-0.04
345	A3	10.70	0.29	0.19	395	A4	9.56	0.91	0.46
346	A0	12.03	0.33	-0.07	396	A5:	12.10	0.13	0.16
347	F7	9.60	0.57	-0.05	397	F7	11.59	0.55	-0.16
348	A9	9.79	0.26	0.24	398	A9	12.17	0.49	-0.04
349	A4	11.07	0.14	0.20	399	A7:	12.16	0.46	-0.15
350	F7	11.97	0.72	0.23	400	F5	11.48	0.65	-0.13

TABLE

No.	Sp.	V	B-V	U-B	No.	Sp.	V	B-V	U-B
401	A2	11.76	0.29	0.19	451	A8	10.19	0.40	0.34
402	F4	9.45	0.50	-0.13	452	A0	11.35	-0.03	0.57
403	F4	11.45	0.51	-0.14	453	A0:	11.19	0.50	0.29
404	A1	10.58	0.13	-0.08	454	A4:	11.40	0.47	0.28
405	F7	10.41	0.53	-0.06	455	A0:	11.34	0.62	0.35
406	F7	10.95	0.61	-0.23	456	F7	11.24	0.50	0.23
407	F4	11.70	0.31	0.03	457	A0	11.45	0.12	0.46
408	F5	10.76	0.58	-0.08	458	A0	11.61	0.22	0.41
409	F5	11.99	0.57	0.25	459	F7	11.57	0.55	0.36
410	F5	9.86	0.63	-0.20	460	F7	11.08	0.40	0.20
411	A7	12.66	0.48	-0.16	461	F5	10.44	0.48	0.08
412	A7	10.86	0.33	0.05	462	A3:	11.59	0.15	0.18
413	F7	11.61	0.68	-0.16	463	F5	11.34	0.56	0.03
414	F6	10.13	0.57	-0.10	464	F1	10.93	0.36	-0.09
415	A1	9.35	0.05	-0.51	465	A0	10.69	0.14	-0.03
416	A0	10.78	0.26	0.00	466	A1	12.10	0.28	0.11
417	F7	11.52	0.61	-0.14	467	A8	11.27	0.39	0.18
418	F7	12.22	0.44	-0.01	468	F6	10.34	0.46	-0.01
419	F7	11.94	0.59	-0.20	469	A1	11.46	0.21	0.05
420	A3	12.23	0.38	0.00	470	F7	12.05	0.48	0.03
421	F7	11.41	0.63	-0.28	471	F7	10.67	0.47	0.14
422	F6	11.54	0.40	-0.02	472	F7	11.79	0.63	-0.08
423	F5	11.10	0.54	-0.19	473	F7	11.97	0.69	-0.03
424	A2	10.12	0.09	-0.14	474	B5	7.17	-0.18	0.18
425	A4:	11.64	0.51	-0.14	475	F7	11.39	0.54	0.06
426	F0:	11.69	0.38	-0.10	476	F5	11.73	0.51	-0.06
427	F5	10.10	0.54	-0.07	477	F3	11.94	0.47	0.04
428	F2	10.62	0.50	-0.21	478	A2	10.90	0.13	0.08
429	F6	9.81	0.43	-0.11	479	F7	12.04	0.56	0.00
430	F3:	12.23	0.45	-0.07	480	F0	10.41	0.29	0.11
431	F7	12.12	0.38	-0.03	481	F7	11.96	0.72	0.05
432	A0	12.03	0.10	0.01	482	F7	11.32	0.50	0.09
433	F7	11.54	0.65	-0.01	483	F7	10.97	0.60	-0.06
434	F6	10.64	0.40	-0.04	484	F7	11.48	0.54	0.10
435	F7	11.95	0.69	-0.21	485	F6	11.89	0.40	0.00
436	F2	11.68	0.61	0.04	486	F5	11.49	0.41	0.17
437	A7:	10.86	0.56	0.03	487	F7	10.93	0.66	-0.07
438	A5	11.59	0.43	-0.01	488	F6	10.87	0.43	-0.06
439	F2	11.15	0.31	0.04	489	F5	11.27	0.33	0.12
440	A5	11.75	0.50	-0.14	490	F7	11.70	0.44	0.26
441	F7	11.78	1.00	0.02	491	A5	11.47	0.28	0.16
442	F7	10.19	0.72	-0.06	492	F7	12.18	0.41	0.13
443	F7	11.56	0.61	0.03	493	F7	10.29	0.45	-0.09
444	A1	10.27	0.28	-0.02	494	F0	10.93	0.26	0.07
445	F7	12.92	0.78	-0.15	495	F7	11.73	0.41	0.13
446	F3	10.09	0.58	0.05	496	F6	8.16	0.27	-0.02
447	A3	10.67	0.49	-0.02	497	F5	11.55	0.43	0.13
448	F7	11.25	0.74	0.01	498	F5	11.70	0.25	0.07
449	A1	11.38	0.39	0.38	499	F4	11.13	0.32	-0.08
450	F2	10.46	0.65	0.04	500	F4	8.31	0.08	0.14

TABLE

No.	Sp.	V	B-V	U-B	No.	Sp.	V	B-V	U-B
501	F2	11.43	0.21	0.10	551	B9	11.92	0.36	0.18
502	F4	10.13	0.29	0.00	552	F1	10.66	0.06	0.55
503	F7	10.83	0.36	0.07	553	F7	11.31	0.29	-0.01
504	F7	10.77	0.49	0.09	554	F6	11.89	0.33	0.13
505	F7	11.44	0.40	0.19	555	F4	11.67	0.37	0.05
506	F5	12.03	0.27	0.23	556	F3	11.60	0.40	0.19
507	A1	12.10	0.06	0.22	557	F7	12.37	0.28	0.22
508	F1	11.39	0.26	0.15	558	A8:	11.70	0.30	0.17
509	A1	10.18	0.01	-0.33	559	A1	10.21	0.05	-0.10
510	F7	10.87	0.47	-0.06	560	F5	10.91	0.46	-0.16
511	A6	11.77	0.25	0.11	561	A7	11.55	0.21	0.26
512	F7	12.16	0.56	0.01	562	F7	11.68	0.09	-0.14
513	A3:	8.85	0.23	0.04	563	F2	9.97	0.46	-0.06
514	A1:	11.98	0.39	0.02	564	F6	11.69	0.45	-0.07
515	F7	10.69	0.00	-0.08	565	A0	9.61	0.10	-0.16
516	F3	11.91	0.32	0.13	566	F4	11.56	0.48	0.03
517	F7	12.18	0.41	0.15	567	F1	9.43	0.39	0.14
518	F6	12.15	0.54	-0.07	568	F7	11.38	0.58	0.18
519	F7	11.18	0.53	0.17	569	A7	9.52	0.36	0.06
520	F4	10.06	0.38	-0.04	570	A3	11.74	0.17	0.18
521	F4	11.31	0.36	-0.06	571	F3	11.13	0.59	0.10
522	A2	11.92	0.12	0.26	572	F7	11.38	0.50	0.05
523	F7	11.61	0.54	0.09	573	F5	8.96	0.41	-0.11
524	F7	10.94	0.39	0.05	574	A3	11.37	0.19	0.07
525	F1	9.99	0.34	0.17	575	A4	9.96	0.41	0.05
526	F1	11.50	0.34	-0.01	576	F6	9.77	0.63	-0.34
527	A0	12.24	-0.04	0.25	577	B5	8.00	-0.07	-0.15
528	F5	12.19	0.35	0.21	578	F6	11.37	0.48	-0.16
529	F7	11.95	0.46	0.06	579	A1	11.41	0.23	0.19
530	A6:	11.94	0.26	0.24	580	A8	9.98	0.31	-0.02
531	F7	11.64	0.46	0.01	581	F7	10.34	0.64	0.03
532	F7	9.82	0.48	-0.24	582	F5	11.12	0.36	-0.15
533	F6	11.07	0.36	0.14	583	F7	12.09	0.47	0.00
534	F7	11.95	0.23	0.16	584	F7	11.20	0.46	-0.04
535	F5	11.98	0.35	-0.08	585	A5	10.27	0.37	-0.04
536	F0	11.57	0.36	0.07	586	B9	9.06	0.01	0.05
537	F5	12.01	0.46	-0.04	587	A0	9.27	0.06	0.01
538	A1	9.53	0.19	0.12	588	F7	10.40	0.36	-0.04
539	F5:	11.97	0.41	-0.08	589	F3	11.01	0.30	-0.16
540	F5	12.23	0.35	0.24	590	F3	11.52	0.67	0.19
541	F2	11.66	0.39	0.09	591	F5	11.12	0.35	-0.17
542	F4	11.30	0.47	0.02	592	B8	9.34	-0.16	-0.02
543	F5	12.05	0.44	0.01	593	A3	11.27	-0.02	0.25
544	F7	11.65	0.55	0.19	594	A7	10.90	0.15	0.11
545	A0	12.66	0.04	0.26	595	F7	12.03	0.26	0.08
546	A3	10.51	0.09	0.22	596	F7	11.68	0.54	-0.19
547	A0	10.08	0.01	0.19	597	F7	11.65	0.39	-0.14
548	F4	11.40	0.39	0.05	598	A7	10.87	0.13	0.04
549	A0	11.73	0.39	0.17	599	A4	11.22	0.27	-0.04
550	A4	11.79	0.26	0.20	600	A7	12.11	0.13	0.13

TABLE

No.	Sp.	V	B-V	U-B	No.	Sp.	V	B-V	U-B
601	F3	8.03	0.34	-0.04	651	F7	9.40	0.50	-0.16
602	F5	10.22	0.45	-0.11	652	A5	11.06	0.20	0.06
603	A8	10.92	0.30	-0.01	653	F2	12.00	0.43	-0.18
604	F6	11.13	0.38	0.06	654	F7	11.54	0.86	0.21
605	F5	11.73	0.30	-0.15	655	F3	11.27	0.49	-0.02
606	F5	9.06	0.34	0.01	656	F7	11.18	0.52	-0.07
607	F0	11.66	0.39	-0.02	657	F5	10.86	0.47	-0.08
608	A8	10.92	0.21	0.23	658	A0	10.98	0.20	0.07
609	A2	10.76	0.18	0.20	659	F4	11.15	0.49	-0.04
610	F7	11.27	0.54	0.09	660	B7	8.58	-0.11	-0.37
611	A4	10.90	0.22	0.07	661	F2	11.49	0.69	-0.16
612	F5	9.07	0.18	0.06	662	F3	9.29	0.44	-0.20
613	F7	9.86	0.38	-0.02	663	A0	9.37	-0.21	-0.16
614	A3	11.24	0.33	0.30	664	F4	10.46	0.26	-0.03
615	F7	11.56	0.40	0.10	665	B9	8.39	-0.25	-0.04
616	F7	11.50	0.26	0.10	666	F6	10.47	0.49	-0.12
617	F7	10.94	0.37	0.07	667	A3	11.52	0.30	0.02
618	A0	9.38	0.07	0.02	668	F5	10.41	0.51	-0.14
619	F3	12.81	0.06	0.13	669	A0	8.95	0.25	-0.15
620	F7	12.06	0.39	0.03	670	F1	9.21	0.27	0.07
621	F0	11.48	0.28	0.02	671	F3	11.29	0.39	0.20
622	A9	11.08	0.18	0.29	672	A9:	11.75	0.29	0.13
623	F7	11.87	0.29	-0.07	673	A1	10.76	0.16	-0.18
624	F6	11.31	0.37	-0.03	674	F7	12.03	0.65	-0.01
625	F7	11.64	0.59	0.07	675	F7	11.58	0.47	-0.11
626	F6	10.93	0.30	-0.03	676	F5	11.88	0.34	0.12
627	F5	12.27	0.18	-0.01	677	A1	10.01	0.00	0.00
628	A5	11.01	0.17	0.17	678	A0	11.54	0.06	0.02
629	F7	13.26	0.50	-0.13	679	F7	11.12	0.46	0.03
630	F2	12.86	0.18	0.10	680	F7	11.55	0.57	0.52
631	A3	10.47	0.09	0.03	681	A0	9.63	0.04	0.08
632	A1	11.26	0.61	-0.42	682	F7	10.24	0.48	0.06
633	A0	9.51	-0.10	-0.03	683	F7	11.25	0.57	0.05
634	F5	10.98	0.30	0.14	684	F5	10.86	0.36	-0.05
635	F7	9.66	0.49	0.09	685	F7	9.53	0.26	0.18
636	A8	11.05	0.07	0.20	686	F7	11.88	0.30	-0.05
637	A0	9.95	-0.19	0.20	687	A3	11.73	0.15	0.35
638	F7	12.18	0.17	0.32	688	F6	11.08	0.34	0.07
639	A7	10.00	0.14	0.16	689	A0	10.54	-0.01	0.14
640	F4	10.79	0.07	0.36	690	A0	10.41	0.05	-0.08
641	A5	11.02	0.28	0.15	691	F0	10.59	0.34	0.04
642	B9	9.08	0.01	0.25	692	A0	11.69	0.37	0.04
643	F4	11.89	0.29	0.17	693	A3	10.92	0.03	-0.13
644	F5	11.56	0.40	0.24	694	F7	9.98	0.78	0.32
645	F3	11.03	0.36	0.06	695	F0	11.68	0.18	0.04
646	F7	10.38	0.75	0.16	696	F3	11.43	0.31	0.05
647	A6	11.10	0.24	0.09	697	F6	7.70	0.31	0.09
648	A0	10.74	0.21	0.22	698	A8	11.50	0.09	0.19
649	F6	9.59	0.47	-0.03	699	F7	11.61	0.26	0.24
650	F6	10.70	0.44	-0.10	700	F4	10.58	0.31	0.00

TABLE

No.	Sp.	V	B-V	U-B	No.	Sp.	V	B-V	U-B
701	F7	11.40	0.53	0.59	751	A0	9.67	0.02	-0.17
702	F2	11.51	0.51	0.13	752	F7	12.08	0.23	0.14
703	F5	12.02	0.48	-0.09	753	A0	12.33	0.41	0.12
704	F2	8.71	0.18	0.07	754	F4	11.29	0.26	0.20
705	A4	10.56	0.15	0.09	755	F6	11.00	0.41	-0.05
706	F5	9.92	0.34	-0.01	756	A4	12.16	0.15	0.40
707	F7	12.06	0.23	0.07	757	F6	11.75	0.48	0.11
708	F7	12.00	0.32	0.06	758	F6	11.18	0.39	-0.05
709	F6	11.54	0.32	0.06	759	F7	11.34	0.35	0.08
710	F3	11.76	0.32	0.04	760	A8:	11.80	0.37	0.20
711	B9	9.72	-0.07	0.07	761	F5	11.85	0.54	0.19
712	A1	9.89	0.10	0.08	762	F6	10.70	0.55	-0.09
713	F3	11.74	0.48	-0.01	763	A1	12.05	0.36	0.12
714	F6	11.46	0.29	0.29	764	A2	11.44	0.36	0.24
715	F7	11.45	0.53	0.05	765	F6	11.13	0.46	0.19
716	F7	10.96	0.54	0.14	766	F7	11.67	0.75	0.30
717	F6	10.22	0.50	-0.16	767	A9	11.16	0.37	-0.01
718	A3:	12.01	0.12	0.08	768	A0	12.26	0.03	-0.13
719	F5	11.58	0.33	0.02	769	A4	10.62	0.19	0.10
720	F2	11.62	0.39	-0.08	770	F7	12.22	0.64	0.01
721	A6	11.64	0.24	0.06	771	F2	11.92	0.34	0.07
722	F4	10.11	0.45	-0.25	772	A1	10.23	0.11	0.05
723	F5	12.06	0.27	0.07	773	F0	11.96	0.17	-0.11
724	F7	12.17	0.40	-0.01	774	A2	12.08	0.53	0.22
725	F7	11.85	0.36	0.02	775	A9	12.26	0.10	0.16
726	F7	11.79	0.40	-0.18	776	F2	10.58	0.33	0.10
727	A1	10.03	0.08	-0.04	777	F7	11.95	0.55	0.03
728	F7	11.26	0.59	-0.07	778	F7	12.05	0.40	0.32
729	F2	9.05	0.35	0.13	779	F7	12.12	0.46	0.00
730	F5	10.28	0.61	0.00	780	A3	12.46	0.32	0.09
731	A4	11.65	0.38	0.33	781	A5	12.61	0.15	0.08
732	A1	10.43	0.26	-0.22	782	F5	11.33	0.38	0.26
733	F7	11.13	0.58	0.03	783	F7	11.48	0.49	0.03
734	A2	11.82	0.32	0.07	784	A7	11.13	0.23	0.25
735	F5	10.25	0.46	-0.08	785	F7	11.93	0.45	0.12
736	F7	12.07	0.57	0.02	786	F7	12.14	0.38	0.13
737	F7	11.79	0.49	-0.04	787	A0	9.82	-0.07	0.24
738	F5	11.36	0.51	0.19	788	A6	10.00	0.15	0.38
739	F6	10.33	0.53	-0.03	789	F7	11.80	0.29	0.19
740	B6:	8.01	-0.11	-0.19	790	F7	11.93	0.41	0.20
741	F7	12.12	0.58	-0.26	791	A5	11.12	0.22	0.22
742	F2	12.01	0.26	0.13	792	F5	11.23	0.39	0.10
743	F1	11.52	0.48	-0.03	793	A9	11.00	0.25	0.08
744	A1	11.25	0.10	0.09	794	F7	11.04	0.53	0.37
745	F7	11.02	0.62	0.19	795	A3	9.28	0.00	0.06
746	F7	11.29	0.64	0.27	796	F2	9.23	0.31	0.24
747	F7	10.91	0.46	0.06	797	F2	9.80	0.39	0.07
748	F7	10.92	0.54	0.10	798	A6	10.87	0.21	0.17
749	F7	11.77	0.46	0.13	799	A7	9.90	0.15	0.26
750	F7	11.48	0.40	0.05	800	F5	11.01	0.23	0.11

TABLE

No.	Sp.	V	B-V	U-B	No.	Sp.	V	B-V	U-B
801	F5	11.00	0.20	0.13	851	A1	11.91	0.18	0.06
802	F7	10.20	0.34	0.14	852	F7	9.66	0.54	-0.20
803	F5	11.81	0.21	0.30	853	F7	11.53	0.75	0.20
804	A0	11.81	0.05	0.27	854	F3	11.63	0.31	0.06
805	F7	11.41	0.41	0.25	855	A5	11.17	0.34	0.04
806	F7	11.32	0.40	0.18	856	F7	13.03	0.75	-0.30
807	F4	11.84	0.31	0.11	857	A0	11.22	0.12	-0.17
808	F6	11.63	0.37	0.21	858	F7	11.11	0.54	-0.01
809	F6	11.44	0.50	0.14	859	F7	11.75	0.44	-0.04
810	F6	10.96	0.36	0.01	860	F7	12.07	0.48	-0.16
811	A5	11.53	0.15	0.20	861	A3	10.93	0.27	0.01
812	F7	9.25	0.23	0.08	862	F6	11.35	0.41	0.27
813	F7	9.37	0.50	0.08	863	F6	10.32	0.58	-0.12
814	F7	11.43	0.71	0.15	864	F7	11.31	0.33	-0.01
815	F7	10.95	0.59	0.11	865	F7	11.73	0.58	-0.22
816	F7	11.35	0.40	0.06	866	F0	10.38	0.51	-0.12
817	B8	8.11	0.11	0.21	867	F7	12.31	0.58	-0.14
818	A3	10.81	0.18	0.17	868	F3	8.09	0.41	-0.17
819	A1	9.21	-0.01	0.03	869	F7	11.59	0.54	-0.49
820	A1	9.78	0.05	0.29	870	F4	11.48	0.44	0.12
821	F6	10.01	0.48	-0.03	871	F7	10.75	0.64	-0.22
822	A2	10.66	0.14	0.13	872	F6	11.87	0.66	-0.16
823	F6	10.65	0.50	-0.04	873	A1	8.67	0.07	-0.05
824	F7	11.77	0.40	-0.09	874	A1	12.78	0.48	-0.17
825	F0	10.97	0.38	0.12	875	F6	9.52	0.58	-0.18
826	F1:	11.57	0.36	0.07	876	F7	12.02	0.49	-0.19
827	F4	11.14	0.37	0.11	877	F7	11.75	0.57	0.07
828	F7	11.64	0.75	0.38	878	F7	12.26	0.67	-0.39
829	F7	11.74	0.33	0.05	879	F7	10.69	0.62	-0.12
830	F6	11.23	0.40	0.02	880	F6	11.76	0.53	0.11
831	F7	12.05	0.46	0.11	881	F5	11.83	0.59	-0.18
832	F7	11.88	0.38	0.11	882	F5	11.03	0.39	-0.01
833	F7	11.80	0.29	0.07	883	F2	8.99	0.40	-0.16
834	F1	10.01	0.48	-0.12	884	B6	8.17	-0.07	0.07
835	F7	11.26	0.84	0.21	885	F7	11.50	0.47	-0.10
836	A8	12.00	0.21	-0.01	886	F5	10.73	0.18	-0.10
837	F6	10.61	0.43	-0.14	887	A6	10.71	0.22	0.13
838	F2	11.72	0.24	0.05	888	A1	12.52	0.32	0.06
839	A9	10.94	0.30	0.18	889	A3	12.31	0.20	0.13
840	F7	10.19	0.73	-0.09	890	A5	11.42	0.29	0.02
841	F4	11.69	0.40	-0.21	891	F7	11.81	0.53	0.18
842	F2	11.33	0.40	-0.02	892	F7	12.11	0.46	-0.20
843	A3	10.51	0.20	0.00	893	A3	10.97	0.07	0.13
844	A4	11.41	0.28	-0.03	894	F6	11.34	0.40	0.09
845	F7	11.78	0.36	0.07	895	F4	11.33	0.26	0.04
846	A1	11.17	0.07	-0.03	896	F7	12.71	0.31	0.13
847	F7	9.84	0.58	-0.05	897	F5	11.51	0.45	0.09
848	A1	11.21	0.12	0.08	898	A2	11.26	0.20	0.12
849	A1	12.12	0.20	0.15	899	A0	10.45	0.22	0.10
850	F5	11.57	0.39	-0.03	900	F6	10.91	0.41	0.10

TABLE

No.	Sp.	V	B-V	U-B	No.	Sp.	V	B-V	U-B
901	F7	11.24	0.54	-0.17	951	F7	11.86	0.80	-0.15
902	B7	8.32	-0.02	-0.07	952	A7	10.06	0.25	0.23
903	A1	12.26	0.26	0.19	953	A7	12.11	0.51	0.19
904	F7	11.95	0.54	-0.13	954	F6	9.88	0.73	0.02
905	F7	11.78	0.45	0.17	955	A4	11.48	0.32	0.16
906	F7	11.58	0.54	0.08	956	F2	10.52	0.43	0.02
907	F6	10.37	0.60	-0.04	957	F4	11.26	0.55	0.03
908	F4	11.67	0.47	0.05	958	F5	11.70	0.64	-0.03
909	F7	11.92	0.52	-0.01	959	A1	11.81	0.31	0.19
910	A6	10.75	0.23	0.71	960	F7	11.02	0.91	0.24
911	F3	10.56	0.44	-0.01	961	A1	11.30	0.13	-0.06
912	A1	10.00	0.24	-0.07	962	F6	11.24	0.61	-0.08
913	F3	11.59	0.31	-0.10	963	A2	11.64	0.43	0.15
914	A0	11.75	0.40	0.02	964	F7	10.98	0.75	0.03
915	F7	11.71	0.39	0.03	965	F7	11.79	0.50	-0.12
916	F6	10.92	0.55	0.01	966	F7	11.63	0.70	0.01
917	A2	11.76	0.11	0.09	967	A1	11.81	0.45	0.14
918	A3	10.96	0.12	0.27	968	F0	12.35	0.47	0.11
919	A1	10.76	0.18	-0.05	969	F0	9.23	0.32	0.08
920	F7	10.45	0.75	0.11	970	F7	9.81	0.75	0.29
921	F7	10.98	0.44	0.06	971	A7	10.23	0.37	0.08
922	F7	9.63	0.63	-0.17	972	A0	11.93	0.29	0.06
923	F6	11.60	0.67	-0.11	973	A9:	12.19	0.41	0.03
924	F7	12.14	0.80	-0.01	974	F6	9.73	0.63	-0.10
925	A2	11.08	0.26	-0.01	975	F7	11.06	0.56	0.00
926	F7	10.66	0.52	-0.01	976	A3:	11.25	0.38	0.00
927	F7	12.13	0.63	-0.19	977	F6	11.40	0.52	0.08
928	F6	11.01	0.48	0.13	978	A8	12.43	0.22	0.27
929	F7	11.59	0.70	0.03	979	F5	9.45	0.27	0.20
930	A7	10.76	0.45	0.01	980	F7	11.65	0.58	0.00
931	F7	11.72	0.76	-0.43	981	F0	9.52	0.35	0.14
932	F7	11.87	0.65	-0.19	982	F7	12.02	0.54	0.37
933	F2	12.01	0.51	-0.05	983	F7	11.89	0.67	0.21
934	F1	10.30	0.43	0.11	984	F7	10.78	0.68	0.07
935	F4	11.22	0.59	0.08	985	A8:	11.19	0.47	0.08
936	F7	11.79	0.58	0.05	986	F7	11.89	0.53	0.21
937	F6	11.24	0.25	-0.06	987	A0	10.76	0.22	0.10
938	F7	11.14	0.60	-0.12	988	F7	11.47	0.50	0.26
939	F3:	12.02	0.30	0.06	989	F6	11.57	0.59	0.18
940	F2	11.36	0.26	0.11	990	F7	12.61	0.42	0.14
941	A1	10.51	0.15	-0.09	991	A0:	12.18	0.33	0.38
942	A1	12.39	0.28	0.12	992	F7	11.00	0.54	0.23
943	F7	11.60	0.51	-0.05	993	F7	11.36	0.51	0.21
944	F7	11.88	0.59	-0.17					
945	A1	10.16	0.18	0.03					
946	F6	10.59	0.26	0.02					
947	A5	10.84	0.28	0.10					
948	F4	11.16	0.42	0.14					
949	F7	12.14	0.49	-0.10					
950	F7	11.67	0.57	-0.09					